Molecular Cell, Vol. 11, 1575–1585, June, 2003, Copyright ©2003 by Cell Press

Structural Basis for Ligand-Independent Activation of the Orphan Nuclear Receptor LRH-1

Elena P. Sablin,[1,3] Irina N. Krylova,[2,3] Robert J. Fletterick,[1] and Holly A. Ingraham[2,*]
[1]Department of Biochemistry and Biophysics
[2]Department of Physiology
University of California, San Francisco
San Francisco, California 94143

Summary

The orphan nuclear receptors SF-1 and LRH-1 are constitutively active, but it remains uncertain whether their activation is hormone dependent. We report the crystal structure of the LRH-1 ligand binding domain to 2.4 Å resolution and find the receptor to be a monomer that adopts an active conformation with a large but empty hydrophobic pocket. Adding bulky side chains into this pocket resulted in full or greater activity suggesting that, while LRH-1 could accommodate potential ligands, these are dispensable for basal activity. Constitutive LRH-1 activity appears to be conferred by a distinct structural element consisting of an extended helix 2 that provides an additional layer to the canonical LBD fold. Mutating the conserved arginine in helix 2 reduced LRH-1 receptor activity and coregulator recruitment, consistent with the partial loss-of-function phenotype exhibited by an analogous SF-1 human mutant. These findings illustrate an alternative structural strategy for nuclear receptor stabilization in the absence of ligand binding.

Introduction

Liver receptor homolog 1 (LRH-1, FTF, NR5A2) and steroidogenic factor 1 (SF-1, AD4BP, NR5A1) are orphan nuclear receptors that define subfamily V of this large gene family. SF-1 and LRH-1 share a high degree of similarity in their DNA binding domains (DBD, 95%) and putative ligand binding domains (LBD, 76%), whereas the large hinge regions separating their DBD and LBD are much less conserved. Both receptors bind DNA with high affinity as monomers, making them distinct from other homodimeric or heterodimeric receptors. SF-1 is required for proper male sexual development (Roberts et al., 1999) and development of endocrine and neuroendocrine tissues (Ingraham et al., 1994; Luo et al., 1994; Parker et al., 2002; Sadovsky et al., 1995; Tran et al., 2003). Although the precise developmental roles for LRH-1 have yet to be defined, both SF-1 and LRH-1 coordinately regulate genes involved in steroid and bile acid/cholesterol homeostasis, respectively (Hammer and Ingraham, 1999; Moore et al., 2002). Expression of SF-1 is high in both the steroid-producing adrenal glands and gonads (Parker et al., 2002), whereas LRH-1 is found in the liver and intestine, where it regulates genes encoding key enzymes in bile acid synthesis, such as CYP7A and CYP8B1 (del Castillo-Olivares and Gil, 2000; Nitta et al., 1999), as well as genes involved in cholesterol transport (Luo et al., 2001; Schoonjans et al., 2002). In instances where SF-1 and LRH-1 are coexpressed, deciphering the specificity of target genes can be difficult because both receptors bind similar sites with equal affinities. Indeed, while SF-1 was assumed to regulate *CYP19* encoding the aromatase enzyme that converts androgen to estrogen (Fitzpatrick and Richards, 1993), expression patterns of these two receptors during follicular maturation showed LRH-1, and not SF-1, as the major regulator of ovarian aromatase (Liu et al., 2003).

The existence of an SF-1 or LRH-1 agonist has not been demonstrated, consistent with the fact that both receptors activate reporter constructs in the apparent absence of ligand. Although oxysterols are proposed to be SF-1 ligands, this hypothesis remains controversial because these steroids fail to alter the activity of SF-1 in most cellular contexts and elicit conformational changes predicted upon ligand binding (Desclozeaux et al., 2002; Lala et al., 1997; Mellon and Bair, 1998). Whether regulation of LRH-1 and SF-1 is ligand independent or is instead achieved by low-affinity, nonspecific ubiquitous ligands, as suggested by some LBD structures (Dhe-Paganon et al., 2002; Stehlin et al., 2001; Wisely et al., 2002), remains an unresolved issue.

For ligand-dependent receptors, hormone binding induces conformational changes that include a critical repositioning of the C-terminal helix H12 within the activation function (AF2) region (Nolte et al., 1998). Similar to other receptors, LRH-1 and SF-1 possess an intact and functional AF2 region (Galarneau et al., 1996; Ito et al., 1997). Further analyses of SF-1 mapped a second activation region (AFH1) to the putative helix H1 in the LBD (Crawford et al., 1997; Desclozeaux et al., 2002). The N-terminal LBD region in LRH-1 and SF-1, including predicted helices H1, H2, and H3, is highly conserved in subfamily V and shares no sequence similarity with other receptor subfamilies (Giguere, 1999). For SF-1, interaction or assembly of this N-terminal region with the remaining portion of the LBD is receptor specific and ligand independent (Desclozeaux et al., 2002). By contrast, assembly of the N-terminal region of ligand-activated receptors with their respective LBDs requires hormone (Pissios et al., 2000). For subfamily V receptors, posttranslational modification of the hinge region just N-terminal to helix H1 provides an additional site for receptor regulation. Indeed, MAPK phosphorylation at serine S203 in SF-1 (LBD begins at Pro224) was found to enhance receptor activity and cofactor recruitment (Desclozeaux et al., 2002; Hammer et al., 1999). Although two potential MAPK phosphorylation sites in the hinge region of LRH-1 have yet to be investigated, stimulation of the MAPK pathway increases LRH-1 activation of the aromatase promoter, implying that LRH-1 activity is also modulated by phosphorylation (I.N.K., unpublished data).

Structural analysis of ligand-dependent receptors has established that ligand-controlled positioning of helix

*Correspondence: hollyi@itsa.ucsf.edu
[3]These authors contributed equally to the work.

H12 in the AF2 region influences recruitment of coregulators, including coactivators and corepressors (Darimont et al., 1998; Glass and Rosenfeld, 2000; Nolte et al., 1998; Shiau et al., 1998). Three-dimensional modeling of the SF-1 LBD suggested that helix H12 in both SF-1 and LRH-1 LBDs would adopt an active conformation in the absence of ligand (Desclozeaux et al., 2002). In vitro data showed that while coregulator binding by SF-1 and LRH-1 appears to be ligand independent, binding affinities are markedly lower compared with ligand-dependent receptors (Hammer et al., 1999; H.A.I., unpublished data), raising the possibility that these coregulators play a less crucial role in SF-1 and LRH-1 function. Tissue-specific repressors for both LRH-1 and SF-1 have been proposed and include the orphan receptors Dax-1 and SHP. The first receptor, Dax-1 is capable of antagonizing both SF-1- and LRH-1-mediated transcription in vitro (Ito et al., 1997; Nachtigal et al., 1998; Suzuki et al., 2003) but is linked more closely with SF-1 by the shared clinical adrenal phenotypes exhibited by *SF-1* and *DAX1* human mutants (Achermann et al., 2001). The second receptor, SHP, also represses both SF-1 and LRH-1 (Lee and Moore, 2002; Suzuki et al., 2003). Targeted deletion in mice of either the *Dax-1* or *SHP* gene partially supports the notion that these two repressors modulate SF-1 or LRH-1 activity, respectively (Kerr et al., 2002; Wang et al., 2001, 2002).

Here, we have undertaken a crystallographic analysis of LRH-1 to determine how subfamily V receptors achieve constitutive activity and whether this activity depends on ligand. In contrast to other nuclear receptors, a stable active monomeric LRH-1 LBD can exist in the absence of ligand, coactivator peptide, or a homo- or heterodimeric receptor partner.

Table 1. Data Collection and Refinement Statistics

Crystallization	
Unit cell dimensions	
a (Å)	34.8
b (Å)	127.5
c (Å)	53.2
β (°)	91.7
Space group	$P2_1$
Molecules per asymmetric unit	2
Resolution (Å)	2.4
Number of unique reflections	17,954
Data redundancy	6
Completeness[a] (%)	98.2 (88.8)
R_{symm}[a,b] (%)	6.7 (16.9)
$< I/\sigma(I) >$	24.4 (5.7)
Refinement (50.0–2.4 Å)	
σ-cutoff	none
R	21.3
R_{free}[c]	23.1
Rms deviation from ideality	
Bond length (Å)	0.009
Bond angle (°)	1.57
Average B factor (A^2)	
All atoms	44.8
Protein atoms	44.6
Water molecules	53.6

[a] Number in parenthesis is for the last resolution shell (2.5–2.4 Å).
[b] $R_{symm} = \Sigma_h|I_h - I|/\Sigma_h I$, where (I) is the mean intensity of reflection h.
[c] R_{free} is for 5% of total reflections.

Results

Crystal Structure of LRH-1 LBD

Crystals of the mouse LRH-1 ligand binding domain were obtained (see Experimental Procedures), and the LRH-1 LBD structure was determined by the molecular replacement method using an atomic model of the hormone-bound RXRα LBD (Egea et al., 2000). The current LRH-1 model consists of residues A318–R559 and was refined to 2.4 Å resolution with R/R_{free} values of 21.3/23.1 (Table 1). LRH-1 shares a common protein fold found in other receptors but contains an additional fourth layer, instead of the typical three-layered sandwich of eleven helices and two short β strands (orange, purple, and pink layers, Figures 1A and 1B). Superposition of LRH-1 with its closest structural relative, hormone-bound RXRα, revealed a conformation that resembles an active, agonist-bound state of ligand-dependent receptors where the C-terminal helix H12 is packed tightly against the H3-H4-H5-H11 region of the LBD (Figure 1C). Furthermore, superposition of Cα atoms from helices H3, H4, H5, H11, and H12 that define the transcriptionally active state of AF2 region showed a rmsd value of 1.0 Å, confirming the active conformation of the LRH-1 LBD.

The LRH-1 structure exhibited three distinct features not present in other LBD structures. The first and most striking feature of LRH-1 is the rigid and relatively long helix H2, which is packed tightly against helix H3 and forms an additional, fourth outer layer in the receptor's structure (Figures 1A and 1B, in red). In most nuclear receptors, as shown here for RXRα (Figure 1C), the region connecting helices H1 and H3 forms a flexible loop that is often partially disordered. The spatial configuration of the extended H2 in LRH-1 contrasts with the short helical fragments termed H2 (and H2′) that have been observed in other nuclear receptor structures (PPARγ, PPARα, PPARδ, RORα, RORβ), where only a loose contact is made with the rest of the receptor's body (Kallen et al., 2002; Nolte et al., 1998; Stehlin et al., 2001; Xu et al., 1999, 2002). The other two related characteristic features of the LRH-1 LBD are the positions of the preceding helix H1 and the N-terminal linker. In LRH-1, helix H1 is translated by one helical turn toward H9 and thus differs from other receptors (Figure 1C). As a consequence of this shift, packing interactions of helix H1 are altered so that the N-terminal proline (P321) is configured on the opposite face of H1 and is likely to influence the direction of the N-terminal linker of LRH-1, which runs along helix H9. We noted that all three LRH-1 structural features are strategically positioned on the outside surface of the LRH-1 LBD (Figures 1A and 1B).

LRH-1 Contains a Large, Well-Formed, but Empty Ligand Binding Pocket

Consistent with the fact that the LRH-1 LBD was expressed in *E. coli* and crystallized without a known natural or synthetic ligand, the structure revealed no ordered ligand in the ligand binding cavity of the receptor (Figure 2A). Nevertheless, the LRH-1 hormone pocket is large (~820 $Å^3$), well defined and fully enveloped or closed by

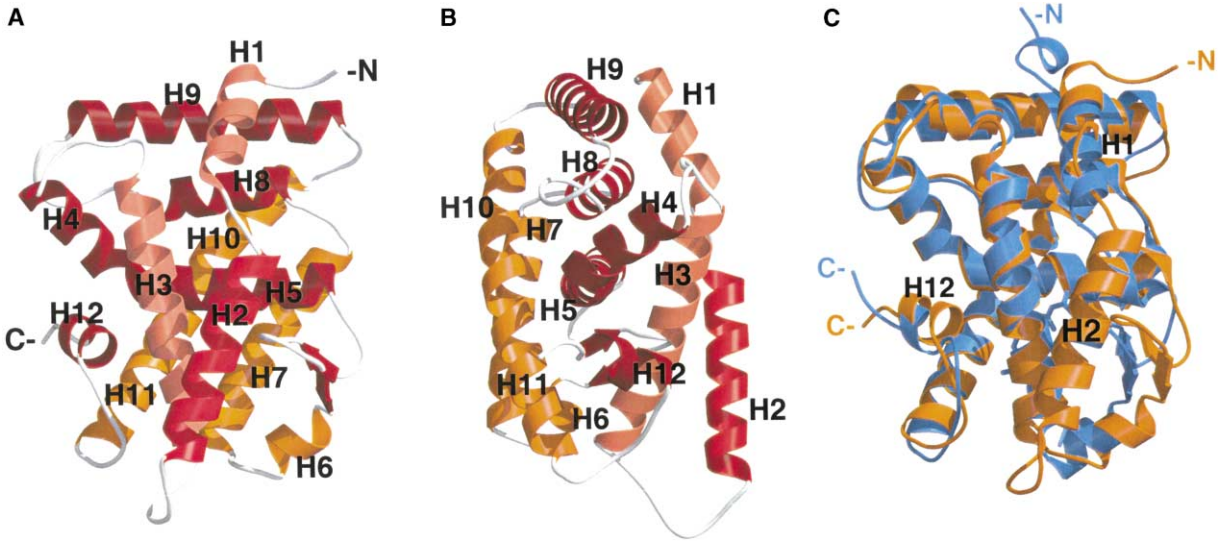

Figure 1. Structure of LRH-1 Ligand Binding Domain

(A and B) Ribbon representation of LRH-1 structure shows α helices and β strands forming four layers in the LRH-1 structure as highlighted with orange, purple, pink, and red, respectively. The view on (B) is rotated ~90° relative to that shown in (A). The LRH-1 specific helix H2 (red) forms the fourth and outmost layer in the structure.

(C) Superposition of LRH-1 with the RXRα LBD bound to ligand (PDB entry 1FBY) depicts LRH-1 in orange and RXRa with 9-*cis*-retinoic acid in blue.

28 amino acid residues lining its walls (listed in the Figure 2 legend). The ligand binding cavity of LRH-1 is mostly hydrophobic but contains one hydrophilic region comprised of three charged residues D408, H409, and a R412, from helix H5. The highly conserved R412 forms a salt bridge with D408. Examination of the pocket by superposition with other liganded structures suggests that the overall shape and size of LRH-1 pocket easily accommodates ligands such as 9-*cis* retinoic acid (Figure 2B) or cholesterol analogs (T. Ayenchi, T. Kuntz, H.A.I, unpublished data). Thus, the overall architecture of the LRH-1 pocket is similar to other ligand-dependent receptors.

The existence of a well-formed cavity within the LRH-1 LBD might imply that a specific ligand is required for modulating receptor activity in vivo, as demonstrated for other orphan nuclear receptors (Greschik et al., 2002; Watkins et al., 2001). To test whether LRH-1 activity might be ligand dependent, single amino acid mutations were created to fill the LRH-1 pocket. Specifically, small side chains facing inside the pocket (A368 and A532 from helices H3 and H11, respectively) were substituted with bulkier residues that would interfere with binding of a putative ligand. The predicted dramatic effect on the size and shape of the LRH-1 ligand binding pocket is illustrated for one such mutant, A368W (Figure 2D). Unexpectedly, we found that all four mutants including A368W, A368M, A532W, and A532M exhibited activity comparable to that of wild-type LRH-1 when tested in HepG2 liver cells, which express active LRH-1 (Galarneau et al., 1996) (Figure 2E). While designed variants rarely improve on nature, we found that H11 pocket mutants (A532W, A532M) exhibited consistently higher activity than wild-type or H3 mutant receptors (Figure 2E). The increased activity of H11 mutants might reflect further stabilization of LRH-1 structure via additional hydrophobic interactions contributed by altered side chains of helix H11, which is normally more rigid than H3. Activities of all four pocket mutants were repressed after cotransfecting the orphan nuclear receptor SHP; however, higher levels of SHP were required to achieve repression in both H11 mutants (Figure 2E). Similar results were obtained in a mammalian two-hybrid system using Gal4-LRH-1 pocket mutants, when tested with either an activated SHP (VP16-SHP) or the coactivator GRIP1 (Figures 2F and 2G). Collectively, these data imply that LRH-1 activity is preserved even after disrupting the size and shape of its ligand binding pocket.

The Monomeric Nature of LRH-1/SF-1

In contrast to nuclear receptors that form homo- or heterodimers, both LRH-1 and SF-1 bind DNA with high affinity as monomers (Galarneau et al., 1996; Nachtigal et al., 1998). Consistent with these data, only monomers were found in the LRH-1 crystals. Furthermore, analytical ultracentrifugation analyses showed that the LRH-1 LBD forms a homogeneous population of monomers in solution (Figure 3A). Because the dimerization interface is topologically conserved in all LBD homo- and heterodimer structures (Gampe et al., 2000; Moraitis and Giguere, 1999; Ribeiro et al., 2001), we created a hypothetical LRH-1 homodimer model by superposing the LRH-1 with LBDs of an active RXRα homodimer. Consistent with our biochemical data, this LRH-1 homodimer model generated a number of steric clashes and repulsive interactions at the virtual dimerization interface. The most dramatic pair of repulsive contacts is generated between two glutamic acid residues, E494 and E513 from helices H9 and H10, respectively (Figure 3B). Remarkably, E513 at the beginning of H10 is a family-specific substitution for the small noncharged residue commonly found in all dimeric receptors (G in RXRα, Figure 3C).

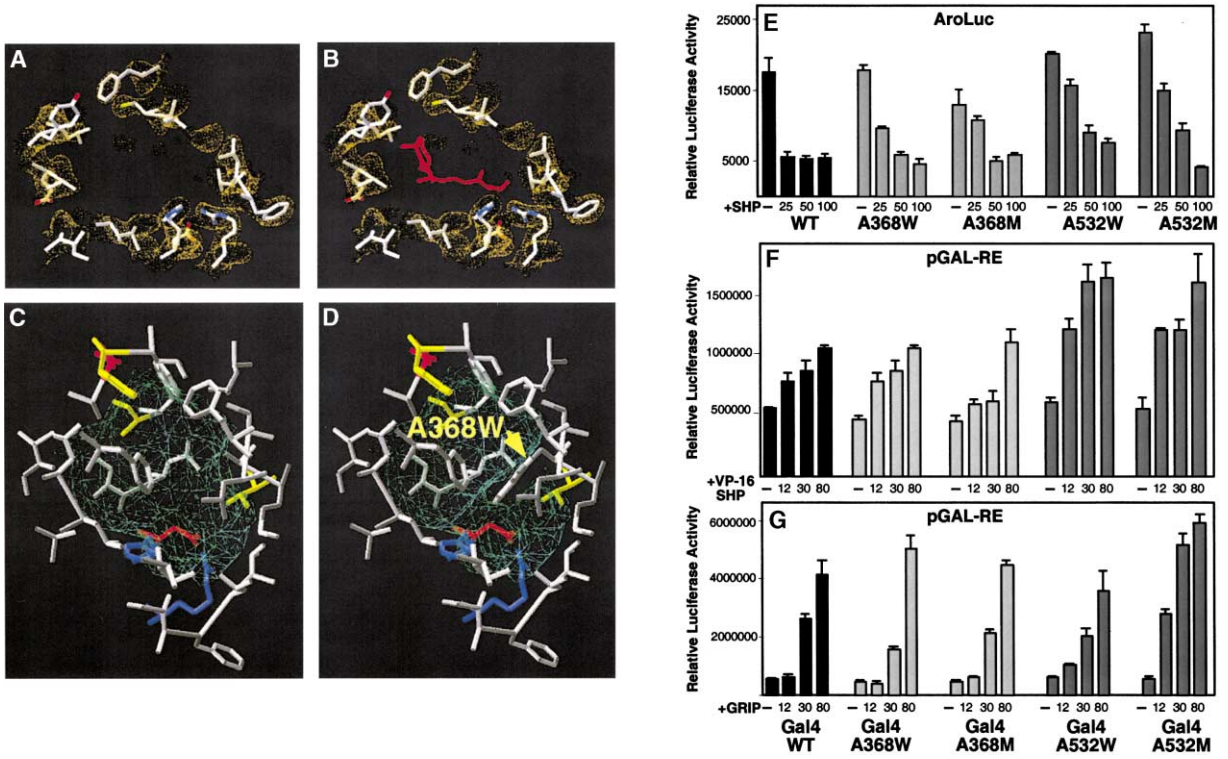

Figure 2. Architecture of LRH-1 Ligand Binding Pocket

(A) A fragment of electron-density map corresponding to the ligand binding pocket of LRH-1 is shown. A simulated annealing composite omit map based on coefficients 2Fo-Fc was calculated for the refined model and is displayed at 1.0 σ in yellow. Residues forming the walls of the ligand binding pocket with corresponding electron density are shown. The 28 residues lining the pocket are (H3) F361, L364, C365, M367, A368, T371; (H5) W401, S402, L405, I406, D408, H409, R412; (S1) I422, F423, L424, V425; (H6) I435; (H7) F443, L446, L447, A450; (H11) I528, A532, E533, Y539, L536; (H12) L551. The small islands in the vicinity of charged residues, as observed in the electron density maps, are most likely water molecules.

(B) An approximate position and size of a hypothetical ligand inside the LRH-1 pocket is indicated by 9-*cis*-retinoic acid (in red) from the liganded structure of RXRa LBD superposed with that of LRH-1.

(C) Hydrophobic and polar residues lining the pocket are depicted as gray and yellow, and positively and negatively charged residues are illustrated in red and blue, respectively. The shape of the enveloped cavity of the pocket is indicated by the green surface.

(D) Mutations inside the LRH-1 ligand binding pocket and their effect on the shape and size of the pocket are shown for one mutant (A368W).

(E) Each LRH-1 pocket mutant was tested in HepG2 cells using the Aroluc reporter construct (200 ng per well); activity is indicated on the *y* axis and was measured either alone (−) or with increasing amounts of the repressor, SHP, as indicated on the *x* axis. Activity is shown as relative luciferase activity using the AroLuc reporter construct containing the proximal promoter of the rat *cyp19* (aromatase) gene.

(F and G) The mammalian Gal4 two-hybrid system was used to test the activity of LRH-1 mutants. All LRH-1 constructs (minus the DBD) were fused to the Gal4 DBD and tested for activation of the pGAL-RE (Gal 4 reporter containing 4 Gal4 binding sites) in HepG2 cells, in the presence or absence of either the mouse corepressor SHP fused to VP16 (+VP16-SHP) or with the human coactivator GRIP1 (+GRIP).

Assuming that E494 and E513 are charged, these repulsive contacts alone would be sufficient to destabilize a homodimer. Destabilization of any canonical heterodimer is also expected because of similar repulsive interactions between the highly conserved E494 in H9 and E513 in H10 of LRH-1 (Figure 3C). While additional LRH-1/SF-1-specific residues could contribute to this distinct feature of subfamily V receptors, the apparent repulsive interactions reported here are sufficient to account for the monomeric states of LRH-1 and SF-1.

Architecture of the Coactivator Binding Cleft of LRH-1

To determine how LRH-1 promotes coactivator binding, we evaluated the fit of the GRIP1 NR-box 2 peptide in the coactivator binding cleft by computational modeling and found that the LRH-1 LBD appears competent to bind a LXXLL coactivator peptide (blue helix, Figure 4A). However, helix H12 is shifted slightly toward the coactivator binding groove in LRH-1, with an rmsd value of 1.5 Å compared with H12 in the RXRα/GRIP peptide complex (Figure 4A). More importantly, optimal peptide docking to LRH-1 could be achieved only after adjustment of side chains in four LRH-1-specific residues that include R380 (H3), Q398 and M394 (H4), and N549 (H12) (Figure 4B). R380 (lysine in other receptors) would be part of the so-called "electrostatic clamp" that stabilizes the receptor-coactivator complex (Darimont et al., 1998). The shorter and uncharged side chain of Q398 in LRH-1 versus those of arginine or lysine found in other receptors could be insufficient to stabilize the position of the C-terminal of H12. The other two residues M394 and N549 have bulkier side chains that could potentially interfere with coactivator docking and are not the usual

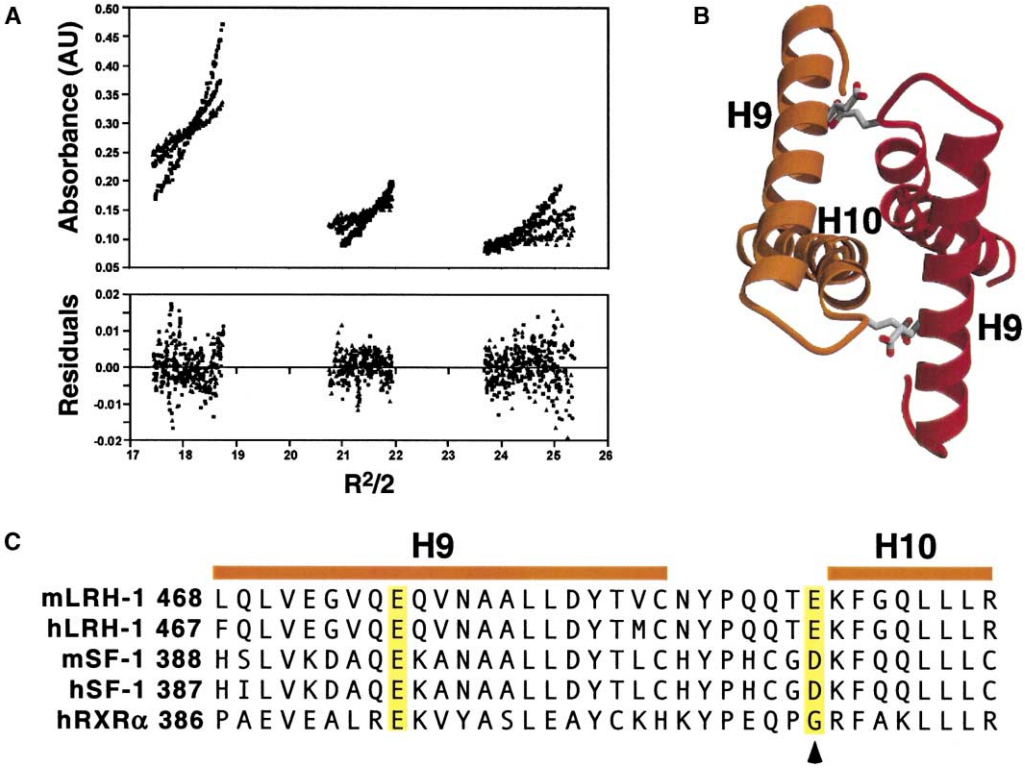

Figure 3. Structural Determinants of LRH-1 Oligomerization State

(A) The sedimentation equilibrium profiles for LRH-1 at different concentrations (8, 4, and 2 μM) are shown with absorbance detected at 277 nm as a function of radial position (upper panel), collected after 19 hr at 8,500 rpm (▲), 12,000 rpm (●), and 17,000 rpm (■). Data were fitted to a single-species model, and the resulting apparent molecular weight (28.4 kDa ± 1.8) corresponds to the calculated weight of the LRH-1 monomer.

(B) Hypothetical LRH-1 homodimerization interface is modeled for two LRH-1 ligand binding domains (in orange and red, respectively) based on RXRα active homodimer (PDB ID 1MZN). Repulsive interactions created by amino acid substitutions (G/E, highlighted in [C]) are indicated.

(C) Primary sequence alignment of family-specific amino acids known to participate in nuclear receptor LBD dimerization is shown with critical residues highlighted.

small residues (A/S/T/V/P) present in most receptors. An optimized LRH-1 coactivator cleft was engineered by replacing the two most bulky and least flexible LRH-1-specific residues to match their counterparts in RXRα (M394V/N549T or mCleft). While the basal activity of the mCleft mutant is reduced, activation of this mutant receptor by nuclear receptor coregulators was significantly elevated compared to wild-type receptor. Paradoxically, activation of LRH-1 by the corepressor SMRT was particularly high (Figure 4C), consistent with previous data showing an interaction between SF-1 and SMRT (Hammer et al., 1999). These data suggest that while binding of LRH-1 to known coregulators is ligand independent, it is not fully optimized.

Helix 2 Is Important for Receptor Activity and Coregulator Recruitment

Given that helix H2 indirectly supports the position of H12 in the LRH-1 structure, we examined possible involvement of this novel element in regulating LRH-1 activity. Initially we asked if the external facing residues of H2 might participate in coregulator recruitment. For these experiments, three polar amino acid residues on the solvent-exposed side of H2 (Q336, Q346, and Q347) were substituted with either alanines or histidines (Figure 5A). This triple LRH-1 mutant (Q336A/Q346A/Q347H or mQ3) showed diminished activity in HepG2 cells when cotransfected with either the coactivator AIB1 (Figure 5B) or the corepressor SHP (Figure 5C). These results were supported further by mammalian two-hybrid data showing that interactions of the mQ3 LRH-1 mutant receptor with VP16mSHP and GRIP1 were lessened (Figure 5D and data not shown). Assuming that there is no change in stability of helix H2 in the mQ3 mutant, these data suggest that residues on the exposed surface of H2 provide an additional binding interface for regulatory proteins.

To test the role of internal residues on helix H2 that face H3, we created an R352E mutation that is positioned at the end of helix H2 (Figure 6A) and which mimics the location of the only reported SF-1 human LBD mutation (R255L) (Biason-Lauber and Schoenle, 2000). A partial loss-of-receptor function is suggested by the milder endocrine phenotype displayed by this SF-1 patient compared to more dramatic phenotypes observed in SF-1 DBD mutants. Moreover, the selective loss of adrenal function in this female is consistent with mouse models showing that adrenal, but not gonadal, development is affected by SF-1 gene dosage (Bland et al., 2000). On the basis of the LRH-1 structure, R352E

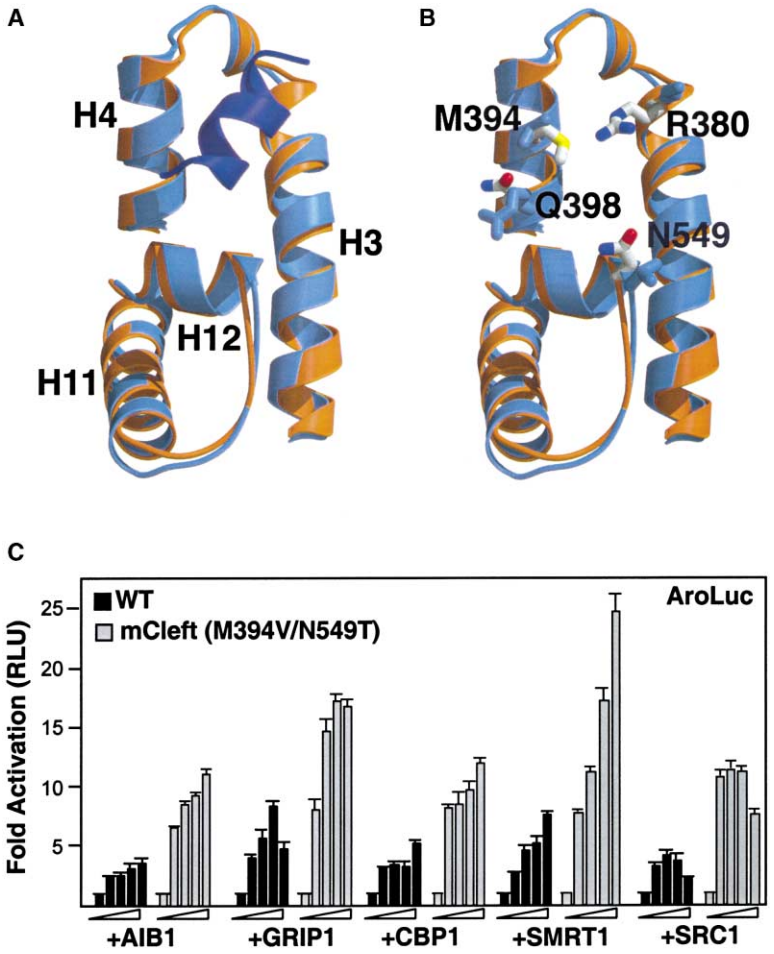

Figure 4. Architecture of LRH-1 Coactivator Cleft

(A) The LRH-1 interface for coactivator binding (orange) is superposed with the corresponding region of active RXRα (PDB ID 1MZN, light blue) complexed with GRIP1 NR box 2 peptide (royal blue). Structural elements forming the interface are indicated.

(B) All family-specific amino acid substitutions at the coactivator binding interface of LRH-1 are highlighted in the atom type-coded colors. Their counterparts in RXRα structure are shown in blue.

(C) Activity of the LRH-1 cleft mutant was assessed in HepG2 cells using the AroLuc reporter (200 ng per well) and is shown as fold activation above basal activity, which is taken to be 1 (first bar in series). For each condition, increasing amounts (12, 30, 80, 200 ng per well) of pcDNA3-hAIB1, pSG5-GRIP1, RSV-mCBP, pSG5-SMRT, and pSG5-SRC1a were added to either wild-type pCImLRH1 (40 ng, black bars) or the double cleft mutant (Q398R and N549T, gray bars). Basal activity for the double cleft mutant was 50% to 75% that of wild-type LRH-1 receptor.

is not predicted to break helix H2 but instead would alter conformations of the H2-H3 loop and the H11-H12 loop at the base of H12, resulting in helix H12 destabilization. Indeed, when tested in cellular transfection assays, the R352E mutant exhibited diminished activity, with no repression by SHP and lowered activation by GRIP1 (Figure 6B). These data are consistent with the structural prediction that an incorrectly packed or misplaced H2 destabilizes the active conformation of H12 and thus provide a structural basis for the partial loss-of-function phenotype observed in the R255L LBD SF-1 human mutant.

Discussion

Our study shows the LRH-1 LBD in an active conformation with a large empty hydrophobic cavity and an additional fourth structural layer formed by an extended helix H2 that is not present in other nuclear receptors. For ligand-dependent receptors, hormone binding induces conformational changes that include a critical repositioning of the C-terminal helix H12 to allow for coregulator recruitment. In the LRH-1 structure, proper positioning of helix H12 is achieved in the absence of ligand or coactivator peptide, suggesting a ligand-independent mode of activation. These features place LRH-1, and by analogy SF-1, in a distinct category and suggest that stability of the active LRH-1 LBD conformation is controlled by different mechanisms. We propose that the constitutive activation of LRH-1 and SF-1 is mediated by a subfamily-specific structural element consisting of an extended rigid helix 2, as evidenced by partial loss of activity in the R352E LRH-1 H2 mutant.

Stability of the LRH-1 Active Conformation in the Absence of a Bound Ligand

For many orphan nuclear receptors, the existence of ligands remains controversial. Structural analyses of many so-called "orphan" receptors revealed the presence of fortuitous ligands that copurified with the LBDs (Billas et al., 2001; Dhe-Paganon et al., 2002; Stehlin et al., 2001; Wisely et al., 2002). These low-affinity pseudoligands, together with coactivator peptides, are proposed to stabilize the LBD and prevent it from collapsing during crystallization experiments (Stehlin et al., 2001). In the case of LRH-1, a fully stable and active LBD conformation did not require a psuedoligand, a dimerization partner, or a coactivator peptide. Thus, although the structure of LRH-1 represents an additional LBD structure without a bound ligand (the others include RXRα, PXR, ERR3, PPARδ, PPARγ, Nurr1, and DHR38 [Baker et al., 2003; Bourguet et al., 1995; Greschik et al., 2002; Nolte et al., 1998; Wang et al., 2003; Watkins et al., 2001; Xu et al., 1999]), this ligandless LBD structure

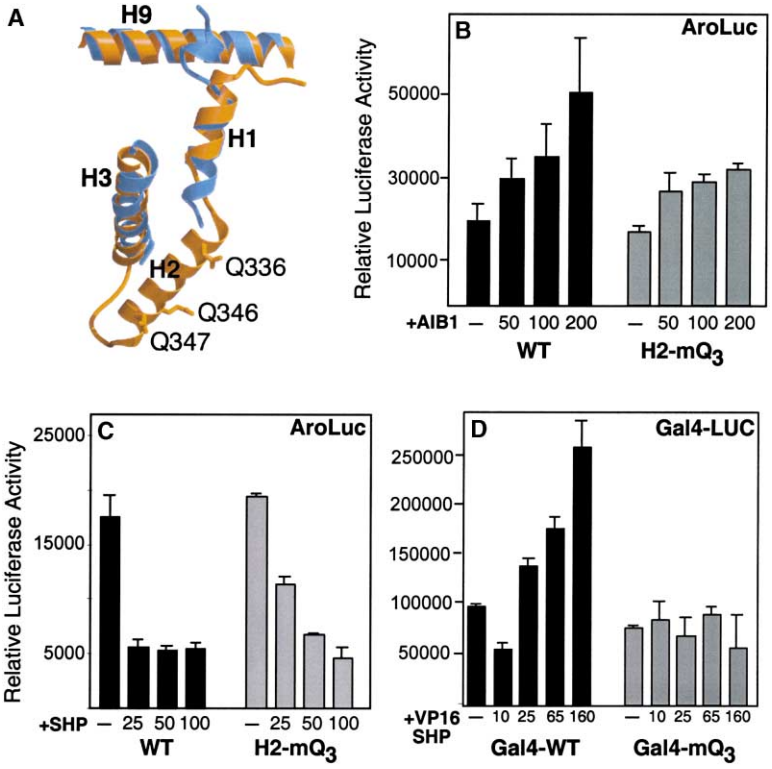

Figure 5. Helix 2 Provides an Interface for Cofactors Recruitment

(A) Ribbon representations are shown for helices 1, 2, 3, and 9 of LRH1 (orange) or RXRα (blue, PDB entry 1FBY), and the positions of the three mutated glutamine residues within H2 of LRH-1 are indicated (Q336A, Q346A, Q347H).

(B and C) The activity of wild-type pCI mLRH1 (black bars) or mQ3 mutant (gray bars, 40 ng) was assessed in HepG2 cells, with or without hAIB1 or mSHP, by measuring Aroluc reporter activity (200 ng per well).

(D) Luciferase activity of pGal-RE-TK (Gal4 reporter) is shown for a mammalian two-hybrid assay employing wild-type Gal4-LRH1ΔDBD (minus DNA binding domain, black bars) or the mQ3 mutant (gray bars) after addition of increasing amounts of VP16 mSHP.

was obtained without any outside (bound coactivator/corepressor peptides, dimerization receptor partners) or inside (ligands, bulky hydrophobic side chains filling the pocket) stabilization factors. Furthermore, for some apo-LBD structures, the ligand binding pocket is solvent accessible or open and therefore filled with solvent molecules that could provide additional stabilization of the pocket, as observed for PXR, ERR3, PPARδ, and PPARγ. The only hormone binding pocket that is fully enveloped or closed, as shown here for LRH-1, is that of the collapsed, inactive apostructure of RXRα. Therefore, to our knowledge, the LRH-1 structure is the first to exhibit an active conformation with a fully enveloped, but unoccupied, hormone binding pocket.

Structural Model for LRH-1 Activation

We propose that in the absence of cognate hormone, the active conformation of LRH-1 LBD is maintained because of the stabilizing effect of the subfamily-specific helix H2 that is packed tightly against the body of

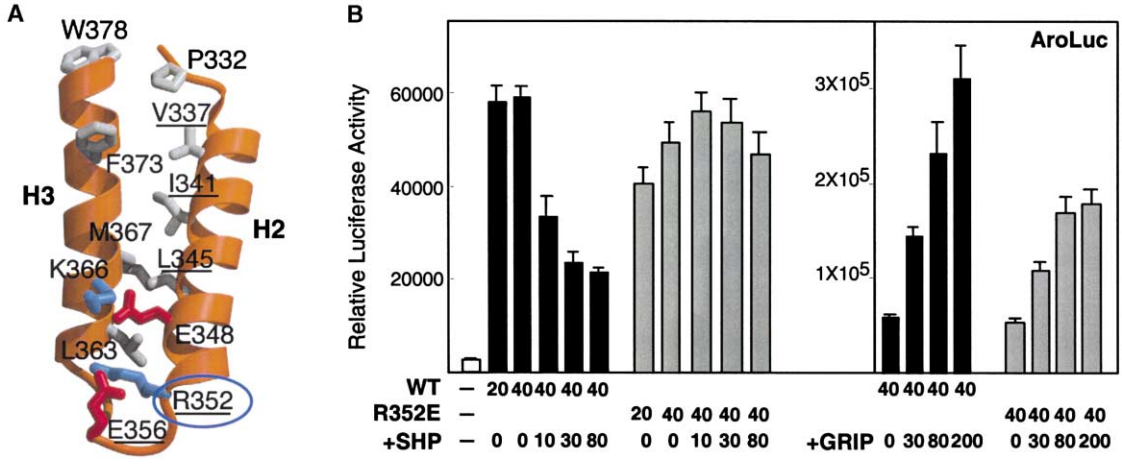

Figure 6. The Role of Helix H2 in Stabilizing and Activating LRH-1

(A) Residues at the interface between helix H2 and H3 are indicated, and those that are conserved between LRH-1 and SF-1 are underlined. The position of the conserved arginine R352 that is mutated in the SF-1 R255L human patient is circled.

(B) Activity of wild-type LRH-1 (black bars) or the R352E mutant (gray bars) was measured using the AroLuc reporter in HepG2 cells, with or without increasing concentrations of mouse corepressor SHP (+SHP) or the coactivator human GRIP1 (+GRIP).

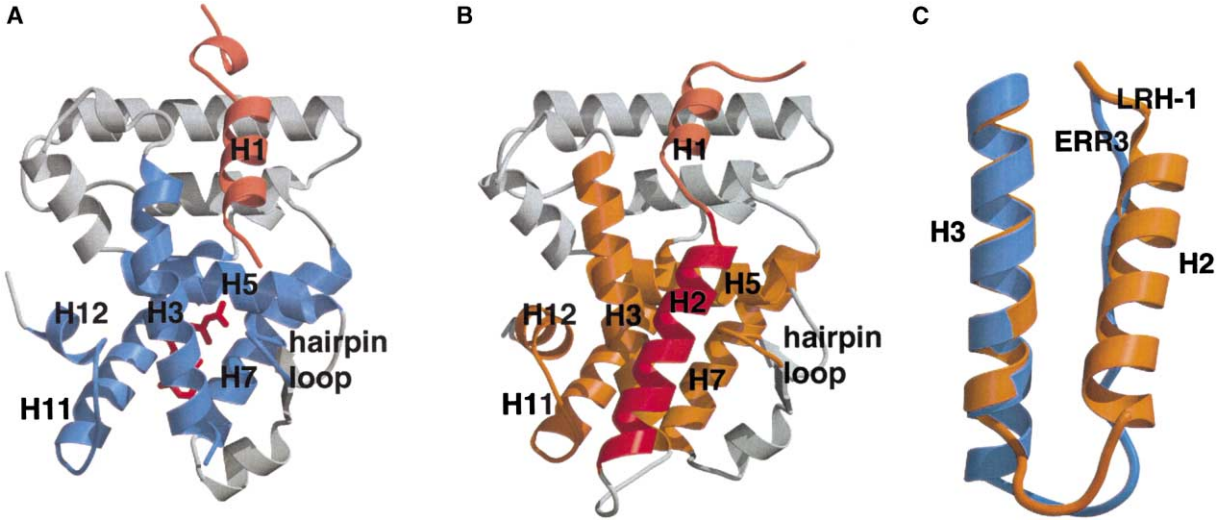

Figure 7. Structural Model for Subfamily V Receptor Activation

(A) Seven structural elements that define the active conformation of ligand-bound RXRα are highlighted in blue (ribbons), with 9 *cis*-retinoic acid shown in red (stick model) (PDB ID 1FBY).

(B) Structural elements of the ligand binding pocket contacted directly or indirectly by helix 2 in the LRH-1 LBD are shown in orange, with helix 2 highlighted in red. Packing interactions of the receptor-specific helix H1 preceding H2 are highlighted in pink for both RXRα (A) and LRH-1.

(C) Superposition of the structural elements of ERR3 (blue, PDB ID 1KV6) with corresponding helices H2 and H3 in LRH-1 (orange ribbons) is shown.

the receptor. On the basis of existing LBD structures, seven structural elements define the hormone binding pocket of the LBD (Steinmetz et al., 2001) (Figure 7A). We find that H2 interacts directly with four structural elements forming the walls of the pocket, including helices H3, H5, the hairpin loop, and the loop connecting H11 and H12 (Figure 7B). Helix H2 helps to define the position of H3 through its extensive packing interactions with H3 that account for an unexpectedly large buried surface (~1200 Å^2). Sequence alignment shows that the interacting faces of helices H2 and H3 are specific to nuclear receptor subfamily V and have likely coevolved to form the observed paired hydrophobic and complimentary electrostatic interactions (Figure 6A). The position of helix H3 is important in that it interacts directly with the remaining three structural elements (H7, H11, and H12) of the pocket. Indeed, loss of activity in the R352E mutant, which is predicted to reposition H3, supports this hypothesis. Thus, we postulate that helix H2 controls both the architecture of the pocket and conformational state of the LBD by either directly or indirectly interacting with all seven elements that define the conformational state of the LBD.

Helix 2 forms a unique fourth, outermost layer in LRH-1 and can be viewed as an integral agonist that functions outside rather than inside the ligand binding pocket. Indeed, cognate ligands and helix H2 exert similar conformational effects on the LBD of the receptor. Like receptor-specific ligands, helix H2 has a defined architecture and a subfamily-specific primary sequence that has coevolved with the interacting surfaces of the LRH-1 LBD. Analogous to specific contacts made by the ligand, packing interactions of this helix with the core structural elements provide sufficient stabilization energy to favor the activated receptor's state in the absence of hormone or coactivator. Although helix H2 is specific for LRH-1 and SF-1, other studies suggest that the region connecting helices H1 and H3 may adopt functionally relevant, receptor family-specific conformations. Recent studies showed that this same region influences the overall stability of the thyroid receptor LBD (Huber et al., 2003). Remarkably, while there is little homology shared between ERR3 and LRH-1 in this N-terminal LBD region, one finds that the nonhelical ERR3 element connecting H1 and H3 (Greschik et al., 2002) follows the path of H2 in LRH-1 (Figure 7C). Thus, we speculate that this rigid connecting region fulfills a similar stabilizing role for ERR3, as H2 does for LRH-1.

Regulation of LRH-1 Activity

While the distinct helix H2 in LRH-1 LBD explains how constitutively active receptors might maintain an active conformation in the absence of ligand, a structural puzzle emerges—do ligands exist for the LRH-1 empty pocket? The existence of a well-formed and large pocket (~820 Å^3) that retains an asymmetrical distribution of electrostatic charge observed in ligand-dependent receptors and is not filled with side chains raises the possibility that natural agonists or antagonists exist for LRH-1. These features of LRH-1 contrast other LBD structures whose bulky side chains either markedly reduce the size of the pocket, as shown for ERR3 (~220 Å^3) (Greschik et al., 2002) or eliminate the pocket completely, as observed for NGF-IB subfamily receptors (Baker et al., 2003; Wang et al., 2003). Because both SF-1 and LRH-1 function in the adult to affect either steroid or bile acid homeostasis, one might easily envision that potential ligands act in a classic feed-forward or feed-back manner. Currently, little evidence exists for such ligands. On the other hand, it is tempting to

speculate that these potential ligands are used selectively in the diverse embryonic and adult functions of SF-1 and LRH-1. Whether the outside stabilizing influences of helix H2 on the LBD represent an earlier or later evolutionary event than ligand binding is unclear. In this regard, others have placed SF-1 and LRH-1 as some of the oldest members of this gene superfamily (De Mendonca et al., 2002; Escriva et al., 2000).

A second puzzle revealed by our study is the finding that the LRH-1 coactivator binding cleft is not fully optimized for common coregulators, which might suggest that modulation by coregulators is less critical for this receptor's function. Indeed, both GST-pull-down assays and direct peptide binding studies show that LRH-1 and SF-1 LBDs exhibit weak binding to common coregulators with little discrimination observed between coactivators and corepressors (Hammer et al., 1999; J. Moore, K. Guy, and H.A.I, unpublished data). On the other hand, these data might suggest the existence of unidentified subfamily V-specific coregulators. Because our analysis was limited to the LBD region of LRH-1, additional domains or modifications within the flexible hinge region, i.e., phosphorylation, might be required for optimal coregulator recruitment by both LRH-1 and SF-1. Future structural analyses of receptor complexes and post-translationally modified receptors, as well as the identification of natural or pharmacological ligands, should provide additional insights into LRH-1 and SF-1 biology.

Experimental Procedures

Plasmids and Cell Transfections

Pf1 plasmid (full-length mouse LRH1/FTF in pCI vector, Promega) was a gift from Dr. Luc Belanger (University of Laval, Quebec) (Galarneau et al., 1996). A DNA fragment encoding mouse LRH-1 LBD residues 313–560 was obtained by PCR using the Pf1 plasmid as template and cloned into the pBH4 plasmid carrying His-6 tag and a cleavage site for TEV protease (gift from Dr. W. Lim, UCSF). All mutant LRH-1 constructs were created using the QuikChange XL Site-Directed Mutagenesis Kit (Stratagene). Expression of each mutant in transfected COS1 cells was shown to be nearly equivalent to wild-type LRH-1 by Western analysis using rabbit anti-LRH-1/FTF antiserum (gift from L. Belanger). LRH1 activity was measured as previously described (Clyne et al., 2002) using the Aroluc reporter, which contains 534 bp of the rat aromatase promoter in pGL2 (Promega). To create the Gal4/mLRH1 fusion construct (Gal4 mLRHΔDBD) for mammalian two-hybrid assay, a Pf1 PCR fragment corresponding to residues 217–560 was cloned into PM1 vector (Clontech). VP16mSHP and CDM8mSHP constructs were a gift from D. Moore (Baylor College of Medicine). The reporter used in the mammalian two-hybrid assay was pGAL-RE-TK described previously (Desclozeaux et al., 2002).

HepG2 human hepatoma cells were grown in DMEM media supplemented by 10% fetal calf serum and were transiently transfected using FuGENE 6 (Roche) according to the manufacturer's protocol. Luciferase expression was assessed using Enhanced Luciferase Assay Kit (BD PharMingen) and Monolight 2010 (Analytical Luminescence Laboratory). Luciferase activities were corrected for transfection efficiency by normalizing to β-galactosidase activity.

Protein Preparation

Protein expression of mouse LRH-1 LBD was induced in BL21(DE3) *E. coli* (Novagen) with 0.2 mM IPTG followed by growth at 18°C for 6 hr. His-tagged LRH-1 LBD protein was purified on a TALON (Clontech) column and eluted in 45 mM of imidazole. After removal of the His-tag with recombinant TEV protease, protein was further purified on a TSKgel Phenyl-5PW column (TOSOHAAS) equilibrated with 0.6 M ammonium sulfate, 1 mM EDTA, and 10 mM DTT and eluted with a 0.6 to 0.0 M ammonium sulfate gradient, followed by chromatography on a MonoQ column (Pharmacia) equilibrated in 20 mM ammonium acetate (pH 7.4), 2 mM CHAPS, 1 mM EDTA, 1 mM DTT. Protein was concentrated in 100 mM of ammonium acetate, 10 mM TCEP, 1 mM EDTA, and 2 mM CHAPS. The protein purity, stability, and homogeneity were assessed using SDS and native PAGE, mass spectrometry (Voyager-DE, PerSeptive Biosystems), gel filtration (16/60 Superdex 75, Pharmacia), and Dynamic Light Scattering (Protein Solutions, DynaPro-MS800).

Analytical Ultracentrifugation

Analytical ultracentrifugation was performed on a Beckman Optima XL-I analytical ultracentrifuge, with detection at 277 nm. LRH-1 LBD protein (8, 4, and 2 uM) was equilibrated at 10°C at three speeds: 8,500, 12,000, and 17,000 rotations per minute in an AnT-50 analytical rotor. The nonlinear least-squares method of the program Nonlin was used to fit multiple data sets to single or multiple species models as previously described (Maluf and Lohman, 2003).

Crystallization, Data Collection, Model Building, and Refinement

Vapor diffusion method was used to obtain crystals of LRH-1 LBD in which 1 μl of protein solution (6 mg/ml) was mixed with 1 μl of reservoir buffer containing 15% glycerol, 21% PEG 4K, 100 mM TRIS (pH 8.8), 5% isopropanol and equilibrated against this buffer for 5–7 days at 15°C. Crystals were cryoprotected using the mother liquor and then flash frozen in liquid nitrogen prior to data collection. X-ray diffraction data were measured at −180°C and collected to 2.4 Å at Advanced Light Source (Lawrence Berkeley National Laboratory) beamline 8.3.1 ($\lambda = 1.1$ Å) using a single crystal. Data were integrated using DENZO and scaled with SCALEPACK. The crystal was of the monoclinic space group $P2_1$ with two ligand binding domains of LRH-1 in the asymmetric unit and cell dimensions of $a = 34.8$ Å, $b = 127.5$ Å, $c = 53.2$ Å, and $\beta = 91.7°$. The LRH-1 LBD structure was determined by the molecular replacement method (package CNS) using atomic coordinates for residues 266–438 (helices 3–11) of the ligand-bound RXRα (Protein Data Bank ID 1FBY). Electron-density maps based on coefficients 2Fo-Fc were calculated from the phases of the initial model. Subsequent rounds of model refinement were performed using programs QUANTA (Molecular Simulations Inc) and CNS, respectively, and the entire structure was checked using simulated annealing composite omit maps. Both LRH-1 ligand binding domains present in the crystal asymmetric unit are virtually identical and include residues A318–R559. The first five N-terminal (Q313–P317) and the last C-terminal (A560) residues are disordered in both LBD domains and not included in the current model. One hundred water molecules are in the asymmetric unit of the current model.

Acknowledgments

We wish to thank Drs. D. Moore, L. Belanger, and M. Suzawa for reagents provided. We also wish to acknowledge Drs. M. Desclozeaux, R. Huber, J. Turner, M. Vinogradova, and H. Der Ou, P. Tsuruda, M. Lee, M. Bland, and M. Suzawa for initial contributions and advice during this project, and J. Holten for help on the beamline 8.3.1. We are especially grateful for the intellectual and technical advice of Giselle Knudsen in the AUC analyses. This work was supported by an NIH program project grant (DK 58390) to R.J.F and H.A.I.

Received: April 7, 2003
Revised: May 28, 2003
Accepted: June 5, 2003
Published: June 19, 2003

References

Achermann, J.C., Meeks, J.J., and Jameson, J.L. (2001). Phenotypic spectrum of mutations in DAX-1 and SF-1. Mol. Cell. Endocrinol. *185*, 17–25.

Baker, K.D., Shewchuk, L.M., Kozlova, T., Makishima, M., Hassell, A., Wisely, B., Caravella, J.A., Lambert, M.H., Reinking, J.L., Krause, H., et al. (2003). The *Drosophila* orphan nuclear receptor DHR38

mediates an atypical ecdysteroid signaling pathway. Cell, in press. Published online May 29, 2003. 10.1016/S0092867403004203.

Biason-Lauber, A., and Schoenle, E.J. (2000). Apparently normal ovarian differentiation in a prepubertal girl with transcriptionally inactive steroidogenic factor 1 (NR5A1/SF-1) and adrenocortical insufficiency. Am. J. Hum. Genet. *67*, 1563–1568.

Billas, I.M., Moulinier, L., Rochel, N., and Moras, D. (2001). Crystal structure of the ligand-binding domain of the ultraspiracle protein USP, the ortholog of retinoid X receptors in insects. J. Biol. Chem. *276*, 7465–7474.

Bland, M.L., Jamieson, C.A., Akana, S.F., Bornstein, S.R., Eisenhofer, G., Dallman, M.F., and Ingraham, H.A. (2000). Haploinsufficiency of steroidogenic factor-1 in mice disrupts adrenal development leading to an impaired stress response. Proc. Natl. Acad. Sci. USA *97*, 14488–14493.

Bourguet, W., Ruff, M., Chambon, P., Gronemeyer, H., and Moras, D. (1995). Crystal structure of the ligand-binding domain of the human nuclear receptor RXR-alpha. Nature *375*, 377–382.

Clyne, C.D., Speed, C.J., Zhou, J., and Simpson, E.R. (2002). Liver receptor homologue-1 (LRH-1) regulates expression of aromatase in preadipocytes. J. Biol. Chem. *277*, 20591–20597.

Crawford, P.A., Polish, J.A., Ganpule, G., and Sadovsky, Y. (1997). The activation function-2 hexamer of steroidogenic factor-1 is required, but not sufficient for potentiation by SRC-1. Mol. Endocrinol. *11*, 1626–1635.

Darimont, B.D., Wagner, R.L., Apriletti, J.W., Stallcup, M.R., Kushner, P.J., Baxter, J.D., Fletterick, R.J., and Yamamoto, K.R. (1998). Structure and specificity of nuclear receptor-coactivator interactions. Genes Dev. *12*, 3343–3356.

del Castillo-Olivares, A., and Gil, G. (2000). Alpha 1-fetoprotein transcription factor is required for the expression of sterol 12alpha-hydroxylase, the specific enzyme for cholic acid synthesis. Potential role in the bile acid-mediated regulation of gene transcription. J. Biol. Chem. *275*, 17793–17799.

De Mendonca, R.L., Bouton, D., Bertin, B., Escriva, H., Noel, C., Vanacker, J.M., Cornette, J., Laudet, V., and Pierce, R.J. (2002). A functionally conserved member of the FTZ-F1 nuclear receptor family from Schistosoma mansoni. Eur. J. Biochem. *269*, 5700–5711.

Desclozeaux, M., Krylova, I.N., Horn, F., Fletterick, R.J., and Ingraham, H.A. (2002). Phosphorylation and intramolecular stabilization of the ligand binding domain in the nuclear receptor steroidogenic factor 1. Mol. Cell. Biol. *22*, 7193–7203.

Dhe-Paganon, S., Duda, K., Iwamoto, M., Chi, Y.I., and Shoelson, S.E. (2002). Crystal structure of the HNF4 alpha ligand binding domain in complex with endogenous fatty acid ligand. J. Biol. Chem. *277*, 37973–37976.

Egea, P.F., Mitschler, A., Rochel, N., Ruff, M., Chambon, P., and Moras, D. (2000). Crystal structure of the human RXRalpha ligand-binding domain bound to its natural ligand: 9-cis retinoic acid. EMBO J. *19*, 2592–2601.

Escriva, H., Delaunay, F., and Laudet, V. (2000). Ligand binding and nuclear receptor evolution. Bioessays *22*, 717–727.

Fitzpatrick, S.L., and Richards, J.S. (1993). *Cis*-acting elements of the rat aromatase promoter required for cyclic adenosine 3′,5′-monophosphate induction in ovarian granulosa cells and constitutive expression in R2C Leydig cells. Mol. Endocrinol. *7*, 341–354.

Galarneau, L., Pare, J.F., Allard, D., Hamel, D., Levesque, L., Tugwood, J.D., Green, S., and Belanger, L. (1996). The alpha1-fetoprotein locus is activated by a nuclear receptor of the Drosophila FTZ-F1 family. Mol. Cell. Biol. *16*, 3853–3865.

Gampe, R.T., Jr., Montana, V.G., Lambert, M.H., Miller, A.B., Bledsoe, R.K., Milburn, M.V., Kliewer, S.A., Willson, T.M., and Xu, H.E. (2000). Asymmetry in the PPARγ/RXRγ crystal structure reveals the molecular basis of heterodimerization among nuclear receptors. Mol. Cell *5*, 545–555.

Giguere, V. (1999). Orphan nuclear receptors: from gene to function. Endocr. Rev. *20*, 689–725.

Glass, C.K., and Rosenfeld, M.G. (2000). The coregulator exchange in transcriptional functions of nuclear receptors. Genes Dev. *14*, 121–141.

Greschik, H., Wurtz, J.M., Sanglier, S., Bourguet, W., van Dorsselaer, A., Moras, D., and Renaud, J.P. (2002). Structural and functional evidence for ligand-independent transcriptional activation by the estrogen-related receptor 3. Mol. Cell *9*, 303–313.

Hammer, G.D., and Ingraham, H.A. (1999). Steroidogenic factor-1: its role in endocrine organ development and differentiation. Front. Neuroendocrinol. *20*, 199–223.

Hammer, G.D., Krylova, I., Zhang, Y., Darimont, B.D., Simpson, K., Weigel, N.L., and Ingraham, H.A. (1999). Phosphorylation of the nuclear receptor SF-1 modulates cofactor recruitment: integration of hormone signaling in reproduction and stress. Mol. Cell *3*, 521–526.

Huber, B.R., Desclozeaux, M., West, B.L., Cunha-Lima, S.T., Nguyen, H.T., Baxter, J.D., Ingraham, H.A., and Fletterick, R.J. (2003). Thyroid hormone receptor-beta mutations conferring hormone resistance and reduced corepressor release exhibit decreased stability in the N-terminal ligand-binding domain. Mol. Endocrinol. *17*, 107–116.

Ingraham, H.A., Lala, D.S., Ikeda, Y., Luo, X., Shen, W.H., Nachtigal, M.W., Abbud, R., Nilson, J.H., and Parker, K.L. (1994). The nuclear receptor steroidogenic factor 1 acts at multiple levels of the reproductive axis. Genes Dev. *8*, 2302–2312.

Ito, M., Yu, R., and Jameson, J.L. (1997). DAX-1 inhibits SF-1-mediated transactivation via a carboxy-terminal domain that is deleted in adrenal hypoplasia congenita. Mol. Cell. Biol. *17*, 1476–1483.

Kallen, J.A., Schlaeppi, J.M., Bitsch, F., Geisse, S., Geiser, M., Delhon, I., and Fournier, B. (2002). X-Ray structure of the hRORα LBD at 1.63 A. Structural and functional data that cholesterol or a cholesterol derivative is the natural ligand of RORα. Structure *10*, 1697–1707.

Kerr, T.A., Saeki, S., Schneider, M., Schaefer, K., Berdy, S., Redder, T., Shan, B., Russell, D.W., and Schwarz, M. (2002). Loss of nuclear receptor SHP impairs but does not eliminate negative feedback regulation of bile acid synthesis. Dev. Cell *2*, 713–720.

Lala, D.S., Syka, P.M., Lazarchik, S.B., Mangelsdorf, D.J., Parker, K.L., and Heyman, R.A. (1997). Activation of the orphan nuclear receptor steroidogenic factor 1 by oxysterols. Proc. Natl. Acad. Sci. USA *94*, 4895–4900.

Lee, Y.K., and Moore, D.D. (2002). Dual mechanisms for repression of the monomeric orphan receptor liver receptor homologous protein-1 by the orphan small heterodimer partner. J. Biol. Chem. *277*, 2463–2467.

Liu, D.L., Liu, W.Z., Li, Q.L., Wang, H.M., Qian, D., Treuter, E., and Zhu, C. (2003). Expression and functional analysis of liver receptor homologue-1 as a potential steroidogenic factor in rat ovary. Biol Reprod., in press. Published online April 2, 2003. 10.1095/biolreprod.102.011767.

Luo, X., Ikeda, Y., and Parker, K.L. (1994). A cell-specific nuclear receptor is essential for adrenal and gonadal development and sexual differentiation. Cell *77*, 481–490.

Luo, Y., Liang, C.P., and Tall, A.R. (2001). The orphan nuclear receptor LRH-1 potentiates the sterol-mediated induction of the human CETP gene by liver X receptor. J. Biol. Chem. *276*, 24767–24773.

Maluf, N.K., and Lohman, T.M. (2003). Self-association equilibria of Escherichia coli UvrD helicase studied by analytical ultracentrifugation. J. Mol. Biol. *325*, 889–912.

Mellon, S.H., and Bair, S.R. (1998). 25-hydroxycholesterol is not a ligand for the orphan nuclear receptor steroidogenic factor-1 (SF-1). Endocrinology *139*, 3026–3029.

Moore, J.T., Goodwin, B., Willson, T.M., and Kliewer, S.A. (2002). Nuclear receptor regulation of genes involved in bile acid metabolism. Crit. Rev. Eukaryot. Gene Expr. *12*, 119–135.

Moraitis, A.N., and Giguere, V. (1999). Transition from monomeric to homodimeric DNA binding by nuclear receptors: identification of RevErbAalpha determinants required for RORalpha homodimer complex formation. Mol. Endocrinol. *13*, 431–439.

Nachtigal, M.W., Hirokawa, Y., Enyeart-VanHouten, D.L., Flanagan, J.N., Hammer, G.D., and Ingraham, H.A. (1998). Wilms' tumor 1 and

Dax-1 modulate the orphan nuclear receptor SF-1 in sex-specific gene expression. Cell *93*, 445–454.

Nitta, M., Ku, S., Brown, C., Okamoto, A.Y., and Shan, B. (1999). CPF: an orphan nuclear receptor that regulates liver-specific expression of the human cholesterol 7alpha-hydroxylase gene. Proc. Natl. Acad. Sci. USA *96*, 6660–6665.

Nolte, R.T., Wisely, G.B., Westin, S., Cobb, J.E., Lambert, M.H., Kurokawa, R., Rosenfeld, M.G., Willson, T.M., Glass, C.K., and Milburn, M.V. (1998). Ligand binding and co-activator assembly of the peroxisome proliferator-activated receptor-gamma. Nature *395*, 137–143.

Parker, K.L., Rice, D.A., Lala, D.S., Ikeda, Y., Luo, X., Wong, M., Bakke, M., Zhao, L., Frigeri, C., Hanley, N.A., et al. (2002). Steroidogenic factor 1: an essential mediator of endocrine development. Recent Prog. Horm. Res. *57*, 19–36.

Pissios, P., Tzameli, I., Kushner, P., and Moore, D.D. (2000). Dynamic stabilization of nuclear receptor ligand binding domains by hormone or corepressor binding. Mol. Cell *6*, 245–253.

Ribeiro, R.C., Feng, W., Wagner, R.L., Costa, C.H., Pereira, A.C., Apriletti, J.W., Fletterick, R.J., and Baxter, J.D. (2001). Definition of the surface in the thyroid hormone receptor ligand binding domain for association as homodimers and heterodimers with retinoid X receptor. J. Biol. Chem. *276*, 14987–14995.

Roberts, L.M., Shen, J., and Ingraham, H.A. (1999). New solutions to an ancient riddle: defining the differences between Adam and Eve. Am. J. Hum. Genet. *65*, 933–942.

Sadovsky, Y., Crawford, P.A., Woodson, K.G., Polish, J.A., Clements, M.A., Tourtellotte, L.M., Simburger, K., and Milbrandt, J. (1995). Mice deficient in the orphan receptor steroidogenic factor 1 lack adrenal glands and gonads but express P450 side-chain-cleavage enzyme in the placenta and have normal embryonic serum levels of corticosteroids. Proc. Natl. Acad. Sci. USA *92*, 10939–10943.

Schoonjans, K., Annicotte, J.S., Huby, T., Botrugno, O.A., Fayard, E., Ueda, Y., Chapman, J., and Auwerx, J. (2002). Liver receptor homolog 1 controls the expression of the scavenger receptor class B type I. EMBO Rep. *3*, 1181–1187.

Shiau, A.K., Barstad, D., Loria, P.M., Cheng, L., Kushner, P.J., Agard, D.A., and Greene, G.L. (1998). The structural basis of estrogen receptor/coactivator recognition and the antagonism of this interaction by tamoxifen. Cell *95*, 927–937.

Stehlin, C., Wurtz, J.M., Steinmetz, A., Greiner, E., Schule, R., Moras, D., and Renaud, J.P. (2001). X-ray structure of the orphan nuclear receptor RORbeta ligand-binding domain in the active conformation. EMBO J. *20*, 5822–5831.

Steinmetz, A.C., Renaud, J.P., and Moras, D. (2001). Binding of ligands and activation of transcription by nuclear receptors. Annu. Rev. Biophys. Biomol. Struct. *30*, 329–359.

Suzuki, T., Kasahara, M., Yoshioka, H., Morohashi, K., and Umesono, K. (2003). LXXLL-related motifs in Dax-1 have target specificity for the orphan nuclear receptors Ad4BP/SF-1 and LRH-1. Mol. Cell. Biol. *23*, 238–249.

Tran, P., Lee, M., Marin, O., Xu, B., Jones, K.R., Reichardt, L.R., Rubenstein, J.L., and Ingraham, H.A. (2003). Requirement of the orphan nuclear receptor SF-1 in terminal differentiation of ventromedial hypothalamic neurons. Mol. Cell. Neuroscience. *22*, 441–453.

Wang, Z.J., Jeffs, B., Ito, M., Achermann, J.C., Yu, R.N., Hales, D.B., and Jameson, J.L. (2001). Aromatase (Cyp19) expression is upregulated by targeted disruption of Dax1. Proc. Natl. Acad. Sci. USA *98*, 7988–7993.

Wang, L., Lee, Y.K., Bundman, D., Han, Y., Thevananther, S., Kim, C.S., Chua, S.S., Wei, P., Heyman, R.A., Karin, M., and Moore, D.D. (2002). Redundant pathways for negative feedback regulation of bile acid production. Dev. Cell *2*, 721–731.

Wang, Z., Benoit, G., Liu, J., Prasad, S., Aarnisalo, P., Liu, X., Xu, H., Walker, N.P., and Perlmann, T. (2003). Structure and function of Nurr1 identifies a class of ligand-independent nuclear receptors. Nature *423*, 555–560.

Watkins, R.E., Wisely, G.B., Moore, L.B., Collins, J.L., Lambert, M.H., Williams, S.P., Willson, T.M., Kliewer, S.A., and Redinbo, M.R. (2001). The human nuclear xenobiotic receptor PXR: structural determinants of directed promiscuity. Science *292*, 2329–2333.

Wisely, G.B., Miller, A.B., Davis, R.G., Thornquest, A.D., Jr., Johnson, R., Spitzer, T., Sefler, A., Shearer, B., Moore, J.T., Willson, T.M., and Williams, S.P. (2002). Hepatocyte nuclear factor 4 is a transcription factor that constitutively binds fatty acids. Structure *10*, 1225–1234.

Xu, H.E., Lambert, M.H., Montana, V.G., Parks, D.J., Blanchard, S.G., Brown, P.J., Sternbach, D.D., Lehmann, J.M., Wisely, G.B., Willson, T.M., et al. (1999). Molecular recognition of fatty acids by peroxisome proliferator-activated receptors. Mol. Cell *3*, 397–403.

Xu, H.E., Stanley, T.B., Montana, V.G., Lambert, M.H., Shearer, B.G., Cobb, J.E., McKee, D.D., Galardi, C.M., Plunket, K.D., Nolte, R.T., et al. (2002). Structural basis for antagonist-mediated recruitment of nuclear co-repressors by PPARalpha. Nature *415*, 813–817.

Accession Numbers

The LRH-1 coordinates have been deposited in the Protein Data Bank under PDB ID 1PK5 and RCSB ID RCSB019382.